RESEARCH PAPER

Investigating the First-Order Flotation Kinetics Models for Iranian Gilsonite

A. Bahrami, F. Kazemi* and J. Abdolahi Sharif

** fatemeh.kazemi70@yahoo.com*

Received: May 2019 Revised: August 2019 Accepted: December 2019

Department of Mining Engineering, Faculty of Engineering, Urmia University, Urmia, Iran.

DOI: 10.22068/ijmse.17.1.11

Abstract: *Kinetic models are the most important instruments to predict and evaluate the performance of flotation circuits. To determine the kinetic order and rate of flotation of a gilsonite sample, flotation experiments were carried out in both rougher and cleaner stages. Experiments conducted using the combinations of petroleum-MIBC, gas oil-pine oil, and one test without any collector and frother. Five first-order kinetic models were applied to the data obtained from the flotation tests by using the Matrix Laboratory software. Statistical analysis showed that the classic first-order model perfectly matched the rougher and cleaner results performed using the petroleum-MIBC combination. The kinetic constants (k) were calculated as 0.04 (s^{-1}) and 0.01 (s^{-1}) for the rougher and cleaner, respectively. Rougher and cleaner tests without collector and frother also matched with the modified gas/solid adsorption and rectangular models with the k values of 0.05 (s^{-1}), and 0.01 (s^{-1}), respectively. The relationship between flotation rate constant, maximum combustible recovery, and particle size were also studied. The results showed that the maximum flotation combustible recovery and flotation rate were obtained with an intermediate particle size both in the rougher and cleaner flotation processes. The combustible recovery and flotation rate in the rougher flotation process were higher than that in the cleaner flotation process.*

Keywords: *Flotation, Kinetics models, Gilsonite, Collector, Frother.*

1. INTRODUCTION

The flotation operation and its associated kinetics and thermodynamics are arbitrary phenomena. The number of particles that permanently adhere to the bubble surface, cause the recovery to be time-dependent. Since the flotation process is theoretically considered as a time-rate recovery process, flotation kinetics can be described using the mathematical models which incorporate both the recovery and rate functions [1, 2]. Various kinetic models are suggested to explain flotation recovery from different aspects. Therefore, the models are complementary to each other. The initial batch flotation model was reported by Garcia-Zuniga [3]. In this work, the differential equation was applied to the kinetics of chemical reaction to describe the process of batch flotation. The general form of the model can be written as:

$$\frac{dc(t)}{dt} = -kc^n \qquad Eq.1$$

The above equation was suggested by Arbiter [4] for the experimental and industrial data in which C is the concentration of particles, t is time, k is flotation rate constant, and n is the kinetic order. Imaizumi and Inoue [5] put forward a new flotation model in which the flotation rate is a continuous distribution of the flotation rates of heterogeneous materials in the cell. Lynch et al. showed that some of the kinetic models did not fit well with the experimental data as some of the minerals float faster than the others [6]. By integrating Eq. 1, the first-order kinetic equation can be written as:

$$C(t) = C(0)e^{-kt} \qquad Eq.2$$

Therefore, the recovery of the valuable mineral is calculated using the following equation:

$$R(t) = 1 - e^{-kt} \qquad Eq.3$$

According to Eq. 3, recovery is an exponential function of time. Negative exponential functions become zero at infinity, so the concentration of particles in the kinetic equation never reaches zero,

[DOI: 10.22068/ijmse.17.1.11]

and the recovery approaches maximum value. This value is called infinite recovery (R∞), and by incorporating it in Eq. 3, it changes to Eq. 4.

$$R_t = R_\infty\left(1 - e^{-kt}\right) \qquad Eq.4$$

Eq. 4 is called standard or classic flotation equation which is the most common and appropriate kinetic model [7]. A great number of flotation models have been proposed to investigate the flotation kinetic behavior [8, 6]. These models have conveniently been defined in three categories: (1) empirical models, (2) probabilistic models, and (3) kinetic models [6]. This paper will consider only conventional kinetic models.

The kinetic study of the flotation process includes all the parameters affecting the concentrate production rate. Concentrate production can be defined in different ways, but in mineral processing, it is introduced as recovery versus time [7]. By combining the separation time with recovery, two major kinetic curves are produced which are called process and kinetic curves [12, 13]. To obtain the flotation kinetic constant and its influence on the flotation circuits, a lot of studies have been conducted. Drzymala et al. carried out a laboratory-scale research on the flotation of different materials and produced some graphs to present the results of the separation process [13]. The separation diagrams included two dimensional with two parameters, one of them is the flotation time and the other is recovery. Based on the results of this research, the kinetic constant is derived by integrating the first-order kinetic equation. Kinetic models can be used to characterize the flotation process. The flotation rate constant f (k) is a function of both the size and hydrophobicity of particles. Though the more commonly used distributions are Delta function as well as rectangular, Kelsall and Gamma models, there is no agreement in the literature on the distribution function which better characterize the floatability distribution [14]. It is clear that various flotation models have been developed on the basis of the processes and sub-processes occurring in flotation. Various approaches have been adopted to quantify the process. Flotation models based on kinetics have prevailed over almost all the flotation conditions regardless of the ore type and ore characteristics as well as flotation cell configurations. It may be concluded that the classical first-order kinetic model is comparatively a better model and can be utilized to optimize the flotation process as it is applicable to both batch and continuous flotation processes with a high confidence level [15]. The first-order models can be used to describe most mineral flotation processes, while there is also evidence that the non-integral-order equation is capable of representing the kinetic characteristics of the batch flotation process [16]. Guanghua et al. proposed a new kinetic model and compared it with four common kinetic models [17]. The kinetic model evaluation showed that the author's model entirely fitted the experimental data. Albijanic et al. focused on the potential application of kinetic models to variable pulp chemical conditions [18]. The flotation tests were performed on a wide range of

Table 1. List of the common kinetic models [5, 7, 9-11]

Series number	Model	Equation
1	Classic first order model	$R_t = R_\infty(1 - e^{-kt})$
2	Klimpel model	$R_t = R_\infty \left\{1 - \frac{1}{kt}(1 - e^{-kt})\right\}$
3	Fully mixed reactor model	$R_t = R_\infty \left\{1 - \left(\frac{1}{1 + \frac{t}{k}}\right)\right\}$
4	Improved gas/solid adsorption model	$R_t = R_\infty \left\{\frac{kt}{1 + kt}\right\}$
5	Second-order model with rectangular distribution of flotability	$R_t = R_\infty \left(1 - \frac{1}{kt}\left(ln(1 + kt)\right)\right)$

[DOI: 10.22068/ijmse.17.1.11]

chemical conditions. The results showed that The Gamma and Kelsall model slightly better-predicted flotation recovery than first-order model with Dirac delta function and Rectangular model for both fixed and variable pulp chemical conditions. The flotation kinetics models for variable pulp chemical conditions might be beneficial in the optimization of flotation circuits.

Gilsonite is a natural bitumen that consists of complex organic compounds, and the flotation process is one of the methods for concentration of gilsonite. Due to various usage of gilsonite, a few studies have been done to determine the flotation parameters of gilsonite. The present study is conducted to determine the kinetic order and parameters of the flotation process performed on a gilsonite sample obtained from Kermanshah province in Iran. In addition, the differences in the flotation kinetics of various size fractions in the rougher and cleaner stages were discussed. Finally, based on the calculated values for the flotation constant and the infinite recovery, the parameters of the flotation processing line were calculated.

2. MATERIALS AND METHODS

2.1. Materials

Asphaltite or gilsonite is a natural bitumen which consists of complex organic compounds. Gilsonite is a black mineral-like obsidian which is brittle and is usually found as a brown micronized powder [19]. The sample investigated in this study was obtained from Geraveh mine of the Kermanshah province in Iran. According to the mineralogical studies, in addition to bitumen, sulfur, non-sulfur, and shale particles were detected as impurities (Fig. 1); Silica, shale, and silt particles were dispersed in the bitumen background, and fine cracks were filled with calcite as a secondary mineral. The main tailing materials in the gilsonite sample were carbonate (calcite and dolomite) and shale compounds, marn, sulfates-like gypsum, fine silica, and opac. The initial ash content of the sample was 35%. Results of sieve analysis and the related ash content are listed in Fig. 2. Also, Table 2 shows the chemical characterization of the gilsonite sample.

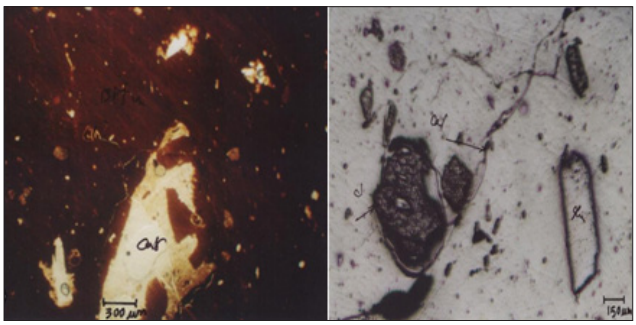

Fig. 1. Photomicrographs of PPL mode of the gilsonite (Car: Carbonate, Bit: Bitumen) (samples from Kermanshah province)

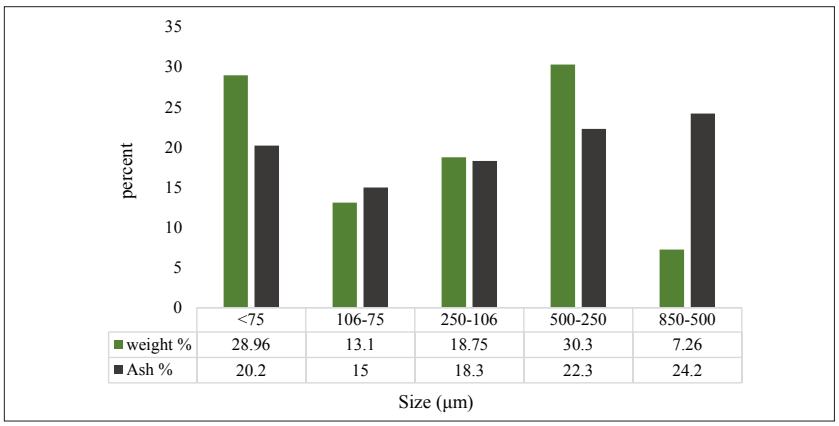

Fig. 2. Ash[1] content of the gilsonite sample in each size fraction

1. In order to determine the amount of ash in a gilsonite sample, 3-4 g of powdered gilsonite particles were burnt in a furnace at 700 ° C for 90 minutes

[DOI: 10.22068/ijmse.17.1.11]

Table 2. Typical properties and elemental compositions of the gilsonite sample

Test	Result	Test method
Moisture content, wt%	≤3	ASTM-D3173[2]
Fixed carbon, wt%	29	ASTM-D3172[3]
Specific gravity 25°c	1.11	ASTM-D3289[4]
Color in mass	Black	-
Color in streak powder	Brown	-
Element Analysis		
Carbon, wt%	74	ASTM-D5291[5]
Hydrogen, wt%	7.1	ASTM-D5291
Nitrogen, wt%	0.67	ASTM-D5291
Oxygen, wt%	3.1	ASTM-D5291
Sulphur, wt%	4	Loco(s, Analyzer)

2.2. Flotation Tests

The flotation reagents were petroleum and gas oil as collectors, MIBC and pine oil as frothers dissolved in tap water. The rougher tests were conducted using three reagent combinations. Firstly, petroleum-MIBC; secondly, gas oil-pine oil; thirdly, test without collector and frother. The rougher tests were performed using two pulp densities with 10% and 25% solid contents. Moreover, the concentrate obtained from the former was subjected to a cleaner stage.

Rougher experiments were conducted using a 4.5 L Denver D12 flotation cell with a 1800 rpm agitation rate. To perform flotation tests, after preparing the feed pulp with defined solid percent, a collector was added to the cell and mixed for 2 min; afterward, frother was also added and mixed for another 30 s. Then the air valve was opened and frothing was done for 200 s. During the operation, the pulp level in the cell was kept constant by replacing the concentrate with tap water.

In order to compare the kinetics parameters of different granulation fractions between two flotation's processes of rougher and cleaner, the operational parameters of the cleaner experiments were like rougher. The cleaner feed was the concentrate obtained from the tests with 10% solid density, but no collector and frother were applied. The final products of all the experiments were divided into six parts according to the frothing periods. 0-20, 20-40, 40-60, 60-80, 80-120, and 120-200 s.

Furthermore, all the products were subjected to sieve analysis using 850, 500, 250, 106, and 75 mesh sieves, and all the fractions were weighed and analyzed for their ash contents. After obtaining the ash content, the flotation recovery was calculated according to the Eq. 5.

$$\%R = \frac{W_c(100 - A_c)}{W_f(100 - A_f)} \qquad \text{Eq. 5}$$

where, Wc is the concentrate weight, Ac is the ash content of the concentrate and Wf and Af are the feed weight and the ash content of the feed, respectively.

3. RESULTS AND DISCUSSION

3.1. Determination of the Kinetic Order of the Rougher and Cleaner Tests

There are two ways to specify the flotation kinetic: (1) obtaining the graph of linear kinetic equations and (2) investigating the dependence of concentration on the initial concentration value [20].

2. Standard Test Method for Moisture in the Analysis Sample of Coal and Coke
3. Standard Practice for Proximate Analysis of Coal and Coke
4. Standard Test Method for Density of Semi-Solid and Solid Asphalt Materials (Nickel Crucible Method)
5. Standard Test Methods for Instrumental Determination of Carbon, Hydrogen, and Nitrogen in Petroleum Products and Lubricants

[DOI: 10.22068/ijmse.17.1.11]

The recovery diagrams of the rougher experiments using different pulp densities, collectors, and frothers are presented in table 3. According to these graphs, achieving 50% recovery in the petroleum-MIBC experiments for both 10 and 25% pulp densities was 20 s. Also, a 50% recovery in the absence of collector and frother was obtained in 20 s. Also, the half time in the gas oil-pine oil test for the pulp samples with 10 and 25% solid content were 10 and 25 s, respectively. Considering the results, the petroleum-MIBC test is first order but the gas oil-pine oil test is not. In the next section, the kinetic parameters of the gilsonite flotation are derived.

Considering the classic, Klimpel, fully mixed reactor model, improved gas/solid adsorption model, and rectangular distribution models, the results of the petroleum-MIBC and in the absence of collector and frother tests at the rougher stage were fitted to the models and the associated parameters were calculated. Fig. 3 indicates that the results of the petroleum-MIBC experiment perfectly fit the classic model and the results obtained in the absence of collector and frother match the modified gas/solid adsorption model. The calculated parameters are presented in Table 4.

It is mentioned that in fitting the kinetics models, firstly kinetics parameters (R and k) were determined by the model fit to experimental data using mathematical software [21].

Table 3. Rougher experiments using petroleum-MIBC, gas oil-pine oil, and in the test absence of collector and frother with 10 and 25 % pulp densities

Recovery of Tests		20 (s)	40 (s)	60 (s)	80 (s)
Petroleum - MIBC	10 % pulp density	50	67.35	72.47	77.89
	25 % pulp density	50	94.98	95.96	98.25
Absence of collector and frother	10 % pulp density	56	67.35	72.47	75.50
	25 % pulp density	56	91.58	94.72	95.96
Gas oil – Pine oil	10 % pulp density	63.05	77.41	84.03	86.05
	25 % pulp density	38.14	75.87	90.35	94.28

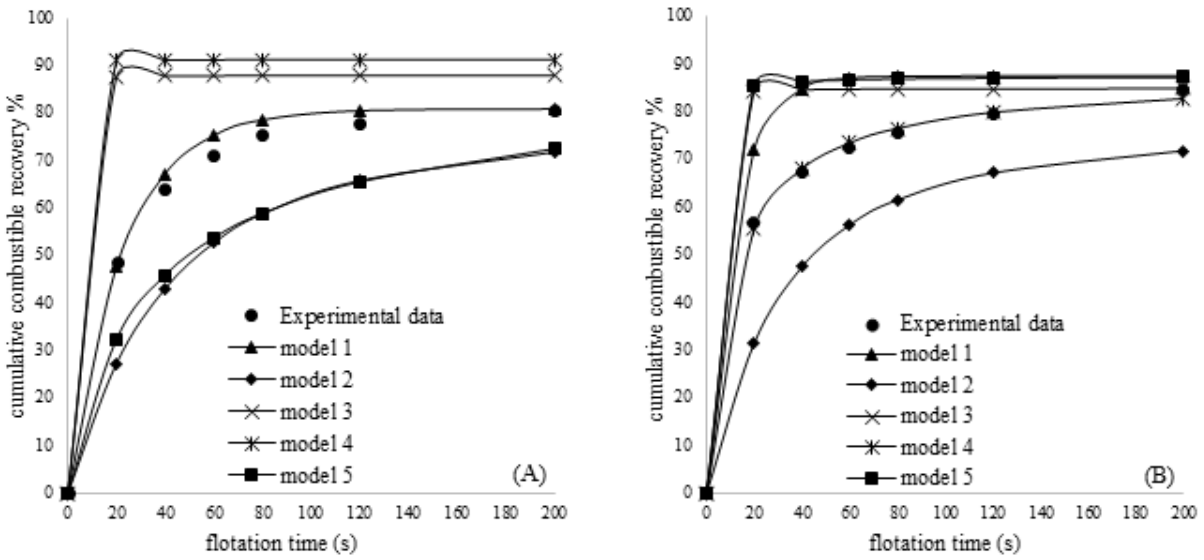

Fig. 3. Fitness of the kinetic models to (A) petroleum-MIBC and (B) absence of collector and frother flotation tests

[DOI: 10.22068/ijmse.17.1.11]

Table 4. Results of the nonlinear regression of the rougher data using first order kinetic models

Models		1	2	3	4	5
Test with Oil collector and MIBC frother	R ∞ (%)	80.89	71.78	87.77	91.16	72.51
	k (s^{-1})	0.04	0.09	15.37	0.06	0.15
	R2	0.99	0.58	0.56	0.42	0.65
Test in the absence of collector and frother	R ∞ (%)	86.69	71.85	86.36	82.76	84.64
	k (s^{-1})	0.05	0.13	11.50	0.08	0.21
	R^2	0.81	0.63	0.73	0.99	0.68

The obtained curves indicate that the kinetic of the oil-MIBC experiment has high compliance with the classic first-order model. Nevertheless, the outcomes of the control test correlate with the improved gas/solid adsorption model. In the rougher flotation experiments using the petroleum-MIBC combination, the kinetic constant is 0.04 (s-1), the retention time is 200 s, and the recovery is 80.89%. These parameters obtained as 0.08 (%), and 82.76%, respectively, for the test performed in the absence of collector and frother. According to table 4, the final recoveries of the petroleum-MIBC test in all of the models are higher than test in the absence of collector and frother. Moreover, the ash content of the flotation concentrates was 24.56 %, and 26.41%, respectively. So, to attain a gilsonite product with lower ash content, the combination of petroleum-MIBC is proposed for the flotation tests.

Fig. 4 illustrates the fitting of first-order kinetic models on the recovery-time data of the cleaner experiments. The obtained curves indicate that the kinetic of the petroleum-MIBC test at the cleaner stage also obeys the classic model. Nevertheless, the outcomes of the tests conducted in the absence of collector and frother in the cleaner stage correlate with the rectangular distribution model. The kinetic constants and final recovery of the cleaner tests are 0.01 (s^{-1}) and 90.8% for the petroleum-MIBC, and 0.02 (s^{-1}) and 76.63% for the test carried out in the absence of collector and frother, respectively. The values of the kinetic parameters related to each kinetic model are presented in table 5.

Comparison of tables 4 and 5 shows that the infinite recovery and flotation constant values in the cleaner process are less than the rougher process. In the rougher process, the percentage of solid pulp is higher than the cleaner process, also the amount of clay and fine-grained impurities in the pulp of rougher is higher, which is due to the phenomenon of entrainment. Some of them are transferred to the froth zone and enter with the concentrate obtains from the flotation cell. During the cleaner process, due to the low

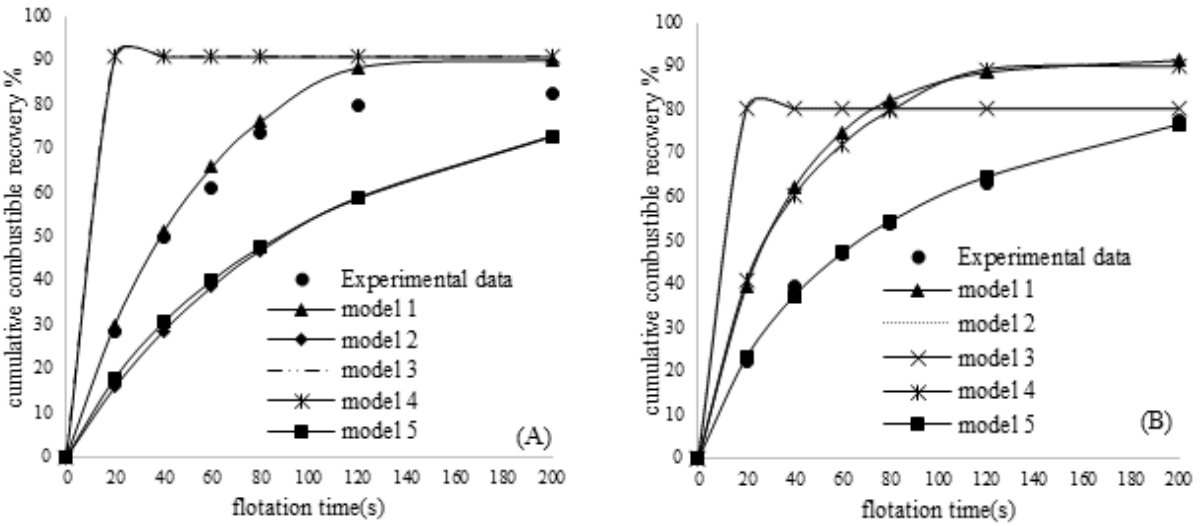

Fig. 4. Fitness of the kinetic models to (a) petroleum-MIBC and (b) absence of collector and frother flotation tests

[DOI: 10.22068/ijmse.17.1.11]

Table 5. Results of the nonlinear regression of the cleaner data using first order kinetic models

Models		1	2	3	4	5
Test with Oil collector and MIBC frother	R ∞ (%)	90.8	73.5	90.08	90.08	72.66
	k (s^{-1})	0.01	0.03	58.32	0.01	0.03
	R^2	0.99	0.45	0.41	0.41	0.49
Test in the absence of collector and frother	R ∞ (%)	90.1	80.26	80.26	90.01	76.63
	k (s^{-1})	0.01	0.02	70.84	0.01	0.02
	R^2	0.20	0.09	0.37	0.20	0.99

density of pulp, the entrainment of clay particles has significantly decreased. Grade of the cumulative concentrate (concentrate produced at 0 to 200 seconds) gained in the rougher and cleaner stages using oil-MIBC experiments are 75.44% and 80.8%, respectively. Also, these values for the test without collector and frother are 73.59% and 76.68%, respectively.

3.2. Effect of Particle Size on the Flotation Kinetic

3.2.1 Rougher Stage

The recovery-time graphs of the flotation experiments using different size fractions are depicted in table 6. As time passes, the recovery increases and then approaches a constant value. The highest recovery is achieved in -250+106 μm fraction that indicates the maximum recovery is obtained for the particles with a medium size. Similar results were reported for the coal flotation [22, 23-2].

Flotation is a physicochemical process that transfers hydrophobic particles to the froth phase using air bubbles. The process is performed in three phases including particle-bubble collision, attachment, and stability [2, 24-23]. Clearly, the particle size is one of the most important factors that affect flotation efficiency.

The flotation recovery of each particle size fraction in the defined time intervals was matched with five first-order kinetic models, and the final results are presented in Fig. 5. Furthermore, the amount of the flotation constant, infinite recovery, and correlation coefficient of each model are calculated and presented in table 7. The maximum recovery of all the models increases by decreasing the particle size. This trend continues to the -250+106 μm fraction, then decreases for -106+75 μm and elevates again for the -75 μm size fraction. These results indicates that the maximum flotation rate constant was also obtained using an intermediate particle size. The results were consistent with those of previous studies [22, 23-2].

It is well known that particle size is an important parameter in the flotation process, and the efficiency of the froth flotation is typically limited to a relatively narrow particle size range [25, 26]. However, out of this range, the recovery drops significantly, whether it is at the fine or the coarse end of the size spectrum [27]. The low combustible recovery of fine particles is mainly because of the poor collision and attachment between the fine particles and air bubbles, whereas the poor combustible recovery of coarse particles is primarily due to the high probability of detachment of the coarse particles from the air bubbles [24, 28-27].

Table 6. Effect of particle size on recovery in the rougher flotation stage using petroleum-MIBC

Size	20 (s)	40 (s)	60 (s)	80 (s)	120 (s)	200 (s)
-850 , +500	10.32	13.77	15.23	16.01	16.38	17.02
-500 , +250	11.98	15.4	16.78	17.55	18	18.57
-250 , +106	15.36	19.71	21.44	22.62	23.09	23.55
-106 , +75	3.78	4.88	5.3	5.3	5.3	5.3
<75	7.27	10.37	12.34	14.08	15.12	16.19

[DOI: 10.22068/ijmse.17.1.11]

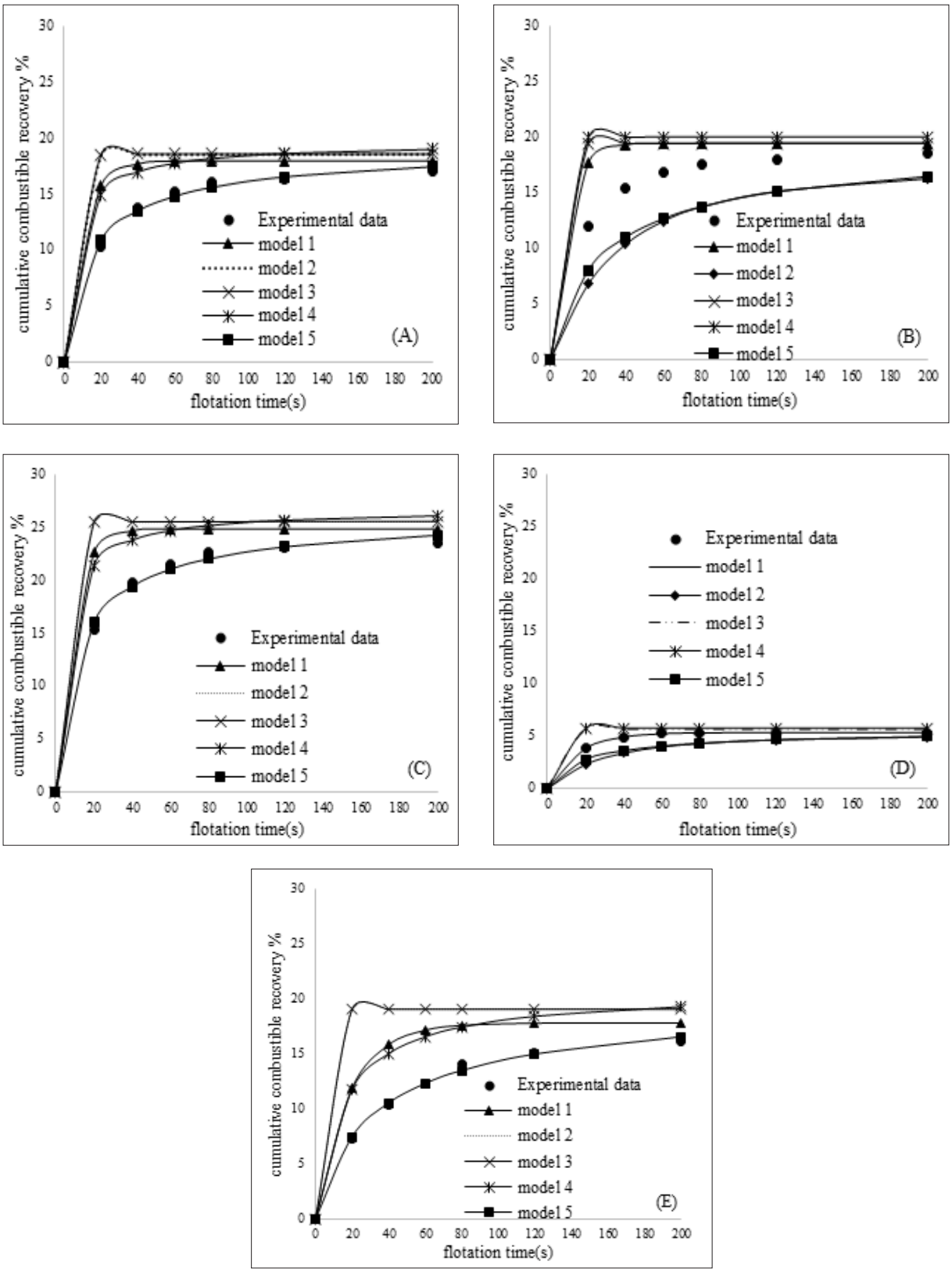

Fig. 5. Fitting the first order kinetic model on the data derived from different size fractions in rougher flotation (A) -850+500, (B) -500+250, (C) -250+106, (D) -106+75, (E) <75 µm

[DOI: 10.22068/ijmse.17.1.11]

Table 7. Results of the non-linear regression of the rougher data using first order kinetic models

Models		1	2	3	4	5
-850+500 μm	R_∞ (%)	16.54	25.50	25.50	18.59	19.57
	$k\ (s^{-1})$	0.05	0.11	12.63	0.07	0.19
	R^2	0.73	0.47	0.47	0.76	0.99
-500+250 μm	R_∞ (%)	18.01	19.45	20.03	20.03	20.96
	$k\ (s^{-1})$	0.05	0.11	12.63	0.07	0.19
	R^2	0.76	0.61	0.68	0.58	0.69
-250+106 μm	R_∞ (%)	23.03	24.84	25.55	25.55	26.72
	$k\ (s^{-1})$	0.05	0.12	12.40	0.08	0.20
	R^2	0.77	0.60	0.60	0.80	0.99
-106+75 μm	R_∞ (%)	5.33	5.68	5.77	5.77	5.96
	$k\ (s^{-1})$	0.06	0.16	8.86	0.11	0.30
	R^2	0.99	0.65	0.80	0.76	0.74
<75 μm	R_∞ (%)	15.92	17.72	19.07	19.07	20.78
	$k\ (s^{-1})$	0.02	0.05	32.16	0.03	0.06
	R^2	0.49	0.01	0.06	0.52	0.99

3.2.2 Cleaner Stage

Table 8 shows the recovery-time curves of the cleaner flotation stage using different particle size fractions. Overall, the variation of the flotation recovery for different size fractions in the cleaner stage is similar to the rougher. The maximum recoveries belong to the -250+106 μm fraction size, and -500+250 μm fraction size portions, respectively that are similar to the rougher stage. The results of the multivariable nonlinear regression on the cleaner flotation of the applied size fractions are presented in Fig. 6 and table 9.

Each size fraction in the cleaner stage correlates with a different kinetic model, and in contrast to the rougher tests, the recovery declines with the particle size. This trend continues till -106+75 μm fraction and then become ascending.

The results suggested that the increases in flotation rates of coarse and fine particle size fractions were especially more obvious than those of the intermediate particle size fractions. It also indicates that the floatability and flotation of gilsonite particles are determined by many factors, such as coal surface properties, particle size, pulp density, and agent concentration [1, 29].

Table 8. Effect of particle size on the recovery of cleaner flotation using petroleum-MIBC

Size	20 (s)	40 (s)	60 (s)	80 (s)	120 (s)	200 (s)
-850 , +500	2.44	5.86	8.96	13.86	18.94	27.59
-500 , +250	6.62	12.32	15.32	19.62	22.43	25.06
-250 , +106	14.4	21.67	24.47	26.59	27.94	28.84
-106 , +75	3.35	5.65	5.65	6.05	6.05	6.05
<75	6.11	8.71	10.85	11.95	13.26	14.77

[DOI: 10.22068/ijmse.17.1.11]

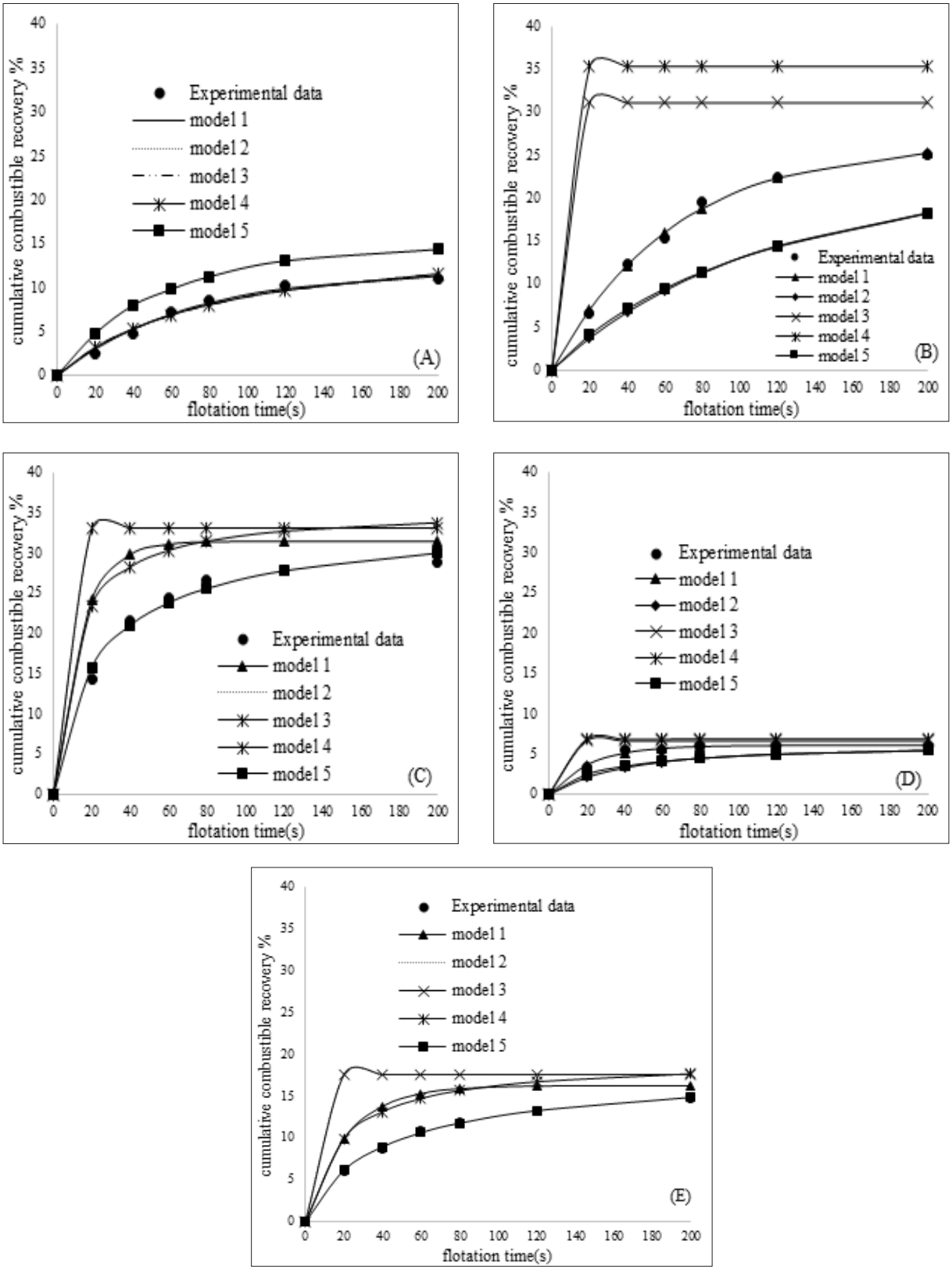

Fig. 6. Fitting the first order kinetic model on the data derived from different size fractions in cleaner flotation (A) -850+500, (B) -500+250, (C) -250+106, (D) -106+75, (E) <75 µm

[DOI: 10.22068/ijmse.17.1.11]

Table 9. Results of the non-linear regression of the cleaner data using first order kinetic models

Models		1	2	3	4	5
-850+500 μm	R ∞ (%)	12.00	14.23	16.37	16.37	18.56
	$k\ (s^{-1})$	0.002	0.003	78.68	0.001	0.002
	R^2	0.99	0.99	0.99	0.99	0.96
-500+250 μm	R ∞ (%)	16.50	17.13	18.35	18.35	20.36
	$k\ (s^{-1})$	0.01	0.02	73.98	0.01	0.02
	R^2	0.99	0.46	0.01	0.02	0.48
-250+106 μm	R ∞ (%)	21.50	23.48	24.14	24.14	25.53
	$k\ (s^{-1})$	0.03	0.07	22.75	0.04	0.09
	R^2	0.61	0.01	0.02	0.63	0.99
-106+75 μm	R ∞ (%)	5.14	5.59	5.60	5.60	5.90
	$k\ (s^{-1})$	0.04	0.10	15.04	0.06	0.16
	R^2	0.99	0.58	0.54	0.43	0.64
<75 μm	R ∞ (%)	14.43	16.28	17.62	17.62	19.37
	$k\ (s^{-1})$	0.02	0.04	38.70	0.02	0.05
	R^2	0.43	0.01	0.01	0.45	0.99

4. CONCLUSION

In this investigation, the difference in flotation rates of various size fractions of Gilsonite between rougher and cleaner flotation processes was studied. Five flotation kinetic models were applied in the fitting process of the flotation data from the rougher and cleaner flotation tests. The MATLAB software was used to estimate the relationship between the flotation rate constant (k), the maximum combustible recovery (R∞), and the particle size based on the nonlinear least-square optimization method. For these purposes, several flotation experiments on a gilsonite sample in different conditions of collector, frother, and pulp densities were studied. According to results, it was concluded that the rougher flotation using the petroleum-MIBC combination and without any collector and frother correlate with the first order kinetic model. Rougher and cleaner data using petroleum-MIBC combination perfectly match the classic first order kinetic model. The k values of these models were 0.04 (s^{-1}) and 0.01 (s^{-1}). On the other hand, the rougher and cleaner experiments without reagents correlated well with the modified gas/solid adsorption, and rectangular models with a k value of 0.05 (s^{-1}), and 0.01 (s^{-1}), respectively. In all of the first order kinetic models, the maximum recoveries were related to the petroleum-MIBC experiments. Also, regarding the recovery values and ash contents of the concentrates, rougher and cleaner stages using petroleum as collector and MIBC as frother were proposed for the gilsonite flotation. Furthermore, the influence of particle size on the recovery and flotation rate of the rougher and cleaner tests using petroleum-MIBC was investigated. In both of the rougher and cleaner experiments, the maximum recovery was associated with the size fractions of -250+106 µm and -500+250 µm, respectively. In the rougher flotation, the kinetic constant and infinite recovery increased by decreasing the particle size, while in the cleaner stage the infinite recovery decreased till the -106+75 µm fraction, and then increased.

REFERENCES

1. Sripriya, R. P. V. T., Rao, P. V. T. and Choudhury, B. R., "Optimization of operating variables of fine coal flotation using a combination of modified flotation parameters and statistical techniques". International Journal of Mineral Processing, 2003, 68, 109-127.
2. Zhang, H., Liu, J., Cao, Y. and Wang, Y., "Effects of particle size on lignite reverse flotation kinetics in the presence of sodium chloride". Powder Techno. 2013, 246, 658–663.
3. Garcia-Zuniga, H., "Flotation recovery is an ex-

[DOI: 10.22068/ijmse.17.1.11]

ponential function of time. Bulletin Minero de la Societal National de Minero", Santiago, Chile 1935, 47, 83–6.
4. Arbiter, N., "Flotation rates and flotation efficiency", Trans. AIME 1951, 791, 796.
5. Imaizumi, T. and Inoue, T., "Kinetic considerations of froth flotation. 6th International Mineral Processing Congress", Cannes 1963, 581-593.
6. Lynch, A. J., Johnson, N. W., Manlapig, EV. and Thorne, C. G., "Mineral and coal flotation circuits, their simulation and control", Elsevier Scientific Publishing Company, 1981.
7. Ek, C., "Flotation kinetics. Innovation in flotation technology". Canada, 1992, 183-210.
8. Mao, L. and Yoon, R. H., "Predicting flotation rates using a rate equation derived from first principles". International Journal of Mineral Processing, 1997, 51, 171-181.
9. Klimpel, R. R., "Selection of chemical reagents for flotation. In: A. L. Mular and R. B. Bhappu (Editors), Mineral Processing Plant Design". AIME, New York, N. Y. 1980, 907-934.
10. Klassen, V. I. and Mokrousov, V. A., An Introduction to the Theory of Flotation, Butterworths, London, 2nd edition, 1963, 493.
11. Trahar, W. J. and Warren, L. J., "The floatability of very fine particles—a review". Int. J. Miner. Process, 1976, 3, 103–131.
12. Jowett, A., "Resolution of flotation recovery curves by a differential plot method". Trans. Inst. Min. Metall, 1974, 85, 263-266.
13. Drzymala, J., Ratajczak, T. and Kowalczuk, P., "Kinetic separation curves based on process rate considerations". Physicochemical problems of mineral processing, 2017, 53, 983-995.
14. Nguyen, A. V. and Schulze, H. J., "Colloidal Science of Flotation". Marcel Dekker, New York 2004, 840.
15. Gharai. M. and Venugopal, R., "Modeling of Flotation Process—An Overview of Different Approaches". Mineral Processing and Extractive Metallurgy Review, 2016, 37, 120-133.
16. Bu, X., Xie, G., Peng, Y., Ge, L. and Ni. Ch., "Kinetics of flotation. Order of process, rate constant distribution and ultimate recovery". Physicochemical Problems of Mineral Processing, 2017, 53(1), 342-365.
17. Guanghua, G., Yang, X. and Li, X., "Flotation characteristics and flotation kinetics of fine wolframite". Powder Technology, 2017, 305, 377–381.
18. Albijanic, B., Subasinghe, N. and Park, C. H., "Flotation kinetic models for fixed and variable pulp chemical conditions". Minerals Engineering, 2015, 78, 66–68.
19. Helms, J. R., Kong, X., Salmon, E., Hatcher, P. G., Schmidt-Rohr, K. and Mao, J., "Structural characterization of Gilsonite bitumen by advance nuclear magnetic resonance spectroscopy and ultrahigh resolution mass spectrometry revealing Pyrrolic and aromatic rings substituted with aliphatic chains". j. of organic Geochemistry, Elsevier, 2012, 44, 21-36.
20. Vapur, H., Bayat, O. and Uçurum, M., "Coal flotation optimization using modified flotation parameters and combustible recovery in a Jameson cell". Energy Conversion and management, 2010, 51, 1891-1897.
21. Wolfarm, S., "The mathematical book". Wolfram Media, Inc. 2003. 22. Welsby, S. D. D., Vianna, S. M. S. M. and Franzidis, J. P., "Assigning physical significance to floatability components". International Journal of Mineral Processing, 2010, 97, 59-67.
23. Muganda, S., Zanin, M. and Grano, S. R., "Benchmarking flotation performance: single minerals". Int. J. Miner. Process, 2011, 98, 182–194.
24. Tao, D., "Role of bubble size in flotation of coarse and fine particles—a review". Sep. Sci. Technol, 2005, 39, 741–760.
25. Gaudin, A. M., Groh, J. O. and Henderson, H. B., "Effect of Particle Size on Flotation". Tech. Publ., 414, American Institute of Mining and Metallurgical Engineering, 1931, 3–23.
26. Shahbazi, B., Rezai, B. and Javad Koleini, S. M., "Bubble–particle collision and attachment probability on fine particles flotation. Chem". Eng. Process. Process Intensify, 2010, 49, 622–627.
27. Jameson, G. J., "Advances in fine and coarse particle flotation". Can. Metall. Q. 2010, 49, 325–330.
28. Schubert, H., "On the optimization of hydrodynamics in fine particle flotation". Miner. Eng. 2008, 21, 930–936.
29. Xia, W., Xie, G., Liang, C. and Yang, J., "Flotation behavior of different size fractions of fresh and oxidized coals". Powder Technol, 2014, 267, 80–85.

[DOI: 10.22068/ijmse.17.1.11]